Monthly Notices
of the
ROYAL ASTRONOMICAL SOCIETY

MNRAS **444,** 1835–1841 (2014) doi:10.1093/mnras/stu1526

The environment of low-redshift quasar pairs

A. Sandrinelli,[1,2,3]★ R. Falomo,[4] A. Treves,[1,2,3] E. P. Farina[5] and M. Uslenghi[6]

[1]*Università degli Studi dell'Insubria, Via Valleggio 11, I-22100 Como, Italy*
[2]*INAF–Osservatorio Astronomico di Brera, Via Emilio Bianchi 46, I-23807 Merate, Italy*
[3]*INFN–Istituto Nazionale di Fisica Nucleare, Sezione Milano Bicocca, Dipartimento di Fisica G. Occhialini, Piazza della Scienza 3, I-20126 Milano, Italy*
[4]*INAF–Osservatorio Astronomico di Padova, Vicolo dell Osservatorio 5, I-35122 Padova, Italy*
[5]*Max Planck Institut für Astronomie, Königstuhl 17, D-69117 Heidelberg, Germany*
[6]*INAF–IASF via E. Bassini 15, I-20133 Milano, Italy*

Accepted 2014 July 28. Received 2014 July 28; in original form 2014 June 9

ABSTRACT

We investigate the properties of the galaxy environment of a sample of 14 low-redshift ($z < 0.85$) quasar (QSO) physical pairs extracted from Sloan Digital Sky Survey Data Release 10 archives. The pairs have a systemic radial velocity difference $\Delta V_{\parallel} \leq 600$ km s^{-1} (based on [O III]5007 Å line) and projected distance $R_{\perp} \leq 600$ kpc. The physical association of the pairs is statistically confirmed at a level of ∼90 per cent. For most of the images of these QSOs we are able to resolve their host galaxies that turn out to be on average similar to those of QSOs not in pairs. We also found that QSOs in a pair are on average in region of modest galaxy overdensity extending up 0.5 Mpc from the QSO. This galaxy overdensity is indistinguishable from that of a homogeneous sample of isolated QSOs at the same redshift and with similar host galaxy luminosity. These results, albeit derived from a small (but homogeneous) sample of objects, suggest that the rare activation of two QSOs with small physical separation does not require any extraordinary environment.

Key words: galaxies: clusters: general – quasars: general.

1 INTRODUCTION

It is widely accepted that all massive galaxies contain a supermassive black hole in their centres. However, only a small fraction of them become active and for a very short time with respect to the evolution time of the galaxies. The mechanism that activates and fuels the nuclei of galaxies is still not well understood. The leading processes thought to be responsible for transforming a dormant massive black hole into a luminous quasar (QSO) are dissipative tidal interactions and galaxy mergers (e.g. Di Matteo, Springel & Hernquist 2005; Callegari et al. 2011, and references therein). Galaxy formation is known to be heavily influenced by the environment, with galaxies in clusters tending to be elliptical and deprived of most of their gaseous content (e.g. Silk & Wyse 1993; Kormendy et al. 2009), and in a number of cases showing signature of interactions and mergers (e.g. Bennert et al. 2008; McIntosh et al. 2008). What is the effective role of these interactions and of the large-scale environment for the triggering and/or fuelling the nuclear activity is not yet clear.

The investigation of QSO environments at various scales (from few kpc to Mpc) and at different cosmic epochs compared with that of normal galaxies still represents an important opportunity to unveil the link between nuclear activity and the immediate environment. The studies of galaxy clustering around QSOs (Stockton 1978; Yee & Green 1984, 1987) and other active galaxies (e.g. Wake et al. 2004) aim to characterize the properties of the environment and to compare them with the environment of non-active galaxies. The emerging picture is not homogeneous. Most of the papers conclude that QSOs reside in regions of galaxy density that are higher than average, albeit with significant difference among various objects. Only in rare cases QSOs are found in relatively rich environments (Stockton 1978; Yee & Green 1984) and the typical environment is a modest group or a poor cluster of galaxies.

Contrasting results emerge when the QSO environments are compared with those of non-active galaxies, depending on the properties of the sample (nuclear luminosity, redshift, radio loudness, etc.). Some differentiation emerges from the comparison of radio loud and radio quiet QSOs. Ellingson, Yee & Green (1991) studied a sample of radio loud quasars (RLQs) and radio quiet quasars (RQQs) at $0.3 < z < 0.6$ and found that the environments around RLQs are significantly denser than those around RQQs. However, Fisher et al. (1996) and McLure & Dunlop (2001) find no difference between the environments of RLQs and RQQs. More recently from the analysis of a large QSO data set at $z < 0.4$ from Sloan Digital Sky Survey (SDSS) Serber et al. (2006) found that the overdensity around the QSOs is larger than that around typical L^* galaxies. However, a more complete comparison of QSOs and inactive galaxies

★ E-mail: asandrinelli@yahoo.it

environments by Karhunen et al. (2014), that includes a matching of the samples in terms of both redshift and galaxy luminosity, shows that the galaxy number density of the QSO environments is comparable to that of the inactive galaxies.

Another important issue about the environment of QSOs is that they are found clustered similarly to galaxies in the local Universe (e.g. Porciani, Magliocchetti & Norberg 2004; Croom et al. 2005, and reference therein). At high redshift the clustering is more difficult to measure but there are indications that its strength would be higher than at the present epoch (e.g. Porciani et al. 2004). The clearest sign of QSO clustering is the finding of QSO pairs, see e.g. the pioneering work of Djorgovski (1991) and the analysis on the Veron-Cetty & Veron (2000) catalogue by Zhdanov & Surdej (2001). Hennawi et al. (2006) found a large sample of QSO pair candidates in a wide range of redshift but a detailed study of the environment was not carried out. Most of these QSO pairs (∼80 per cent) are at $z > 1$ hindering observations of their environment. A number of high-redshift QSO pairs have also been discovered by Hennawi et al. (2010).

Detailed study of the environment of a QSO pair at $z \sim 1.3$ has been reported by Djorgovski et al. (1987). Boris et al. (2007) investigated the environment of four QSO pairs at $z \sim 1$ with separations $\gtrsim$1 Mpc. They found one pair in a particularly high-density region, some evidences for galaxy cluster in the proximity of other two, while one pair appears isolated. A more systematic study was presented by Farina, Falomo & Treves (2011, hereafter F11) for six low-redshift physical QSO pairs from the SDSS data set. They reported a pair in a moderately rich group of galaxies together with dynamical evidence of additional mass to make the pairs bound systems. More recently, Green et al. (2011) searched for signatures of galaxy clusters and hot inter cluster medium associated with seven close ($R_\perp < 25$ kpc) QSO pairs. Because of low-quality images they fail to resolve the host galaxies and to set stringent limits to the galaxy environments. Nevertheless from their observations there is no evidence that these pairs are in rich cluster environments.

Rare examples of QSO associations with more than two objects have been reported (Djorgovski et al. 2007; Farina et al. 2013) but the limited number prevents performance of a statistical analysis.

In this paper, we explore the galaxy environments and the dynamical properties around 14 low-redshift QSO physical pairs derived from SDSS Data Release 10 (SDSS-III DR10, Ahn et al. 2014) spectroscopic and imaging data sets. For these systems, we perform a detailed analysis of their host galaxies and of the clustering of galaxies around the pairs. We are then able to compare the properties of these environments with those of a homogeneous sample of QSOs not in pair spanning the same range of redshift and host galaxy luminosities. Finally, from the difference of systemic velocity of each pair (derived from [O III]λ5007 emission lines, hereafter [O III]) we set constraints on the total minimum mass of the systems based on the dynamic of the pair.

In this work, we assume a concordant cosmology: $H_0 = 70$ km s^{-1} Mpc^{-1}, $\Omega_m = 0.30$ and $\Omega_\Lambda = 0.70$.

2 THE SAMPLE OF QUASAR PHYSICAL PAIRS

We searched for QSO pair candidates from a data set of ∼260 000 QSOs drawn from the SDSS combining the QSO spectroscopic catalogues of Schneider et al. (2010) and of Pâris et al. (2014). We restricted the search to the ∼40 000 QSOs with $z < 0.85$, in order to derive redshifts from [O III] narrow emission line, which is a much better indicator of the systemic velocity of the QSO host galaxy (Hewett & Wild 2010; Liu et al. 2014).

To search for QSO pair candidates we computed the number N_{obs} of QSOs in the catalogue that have $\Delta V_\parallel < \Delta V_{\parallel,limit}$ and $R_\perp < R_{\perp,limit}$, where $\Delta V_{\parallel,limit}$ and $R_{\perp,limit}$ are fixed values, and compared with the number N_{exp} of expected random association using the redshift permutation method (e.g. Zhdanov & Surdej 2001). It consists in maintaining fixed the positions of the QSOs, permuting randomly the redshifts. 10 000 runs were performed. We repeated the search with various value of $\Delta V_{\parallel,limit}$ and $R_{\perp,limit}$ in order to optimize the number of candidates with respect to the number of chance associations. It turns out that the best choice is $R_\perp < 600$ kpc and $\Delta V_\parallel < 600$ km s^{-1}. For this combination, we find 26 QSO pair candidates of which only 3–4 (∼14 per cent) are expected to be false pairs (random associations).

At this stage of the selection $\Delta V_\parallel$ was determined from SDSS redshifts. We inspected the spectra of all candidates to ensure that the systemic $\Delta V_\parallel$ could be reliably derived from [O III] lines. For two dubious classifications we removed two QSO pair candidates, another one for the lack of the [O III] wavelength region in one spectrum. Because of poor signal-to-noise ratio, 8 pair candidates have the [O III] line position hardly measurable for at least one QSO. For the remaining pairs, the [O III] line position was measured with procedure described in F11, where the centroid was evaluated as the median of the barycentres of the line above different flux thresholds and the interquartile range as uncertainty. In one case $\Delta V_\parallel$ from [O III] did not satisfy the condition <600 km s^{-1}, which instead was fulfilled by the SDSS redshifts, and the pair candidate was removed.

In our sample of 14 QSO pairs, we then expect that 1–2 pairs could be chance superpositions. We can assume that the selected sample is mostly composed of physically associated objects where the QSO velocities are due to gravitational binding. The final list of the QSO pair candidates is reported in Table 1 and details on [O III] line measurements are given in Table 2. None of our QSO pairs are present in catalogues of lensed QSOs (CfA-Arizona Space Telescope LEns Survey of gravitational lenses, CASTLE;[1] SDSS Quasar Lens Search, SQLS[2]). Moreover detailed comparison between the spectra of each pair exhibits clear differences that exclude the possibility of gravitational lensing. The redshifts of these QSO pairs are $0.23 \lesssim z \lesssim 0.82$, with $z_{ave} = 0.58 \pm 0.16$. An example of the SDSS spectra of a selected QSO pair is given in Fig. 1.

3 HOST GALAXIES

We retrieved the *i* images of QSO pairs from the SDSS DR10 imaging archive. Analysis was made using the Astronomical Image Decomposition and Analysis software (Uslenghi & Falomo 2008). Our procedure for the study of the QSO host galaxies follows closely that adopted by Falomo et al. (2014) for the imaging study of 400 low-redshift ($z < 0.5$) SDSS QSOs in Stripe 82. In particular, the analysis provides the decomposition of the QSO components, nucleus and host galaxy (see Fig. 2), resulting in 19 QSOs with resolved host galaxies (R), five marginally resolved (M), and four objects unresolved (U); for 10 pairs we are able to characterize the host galaxy properties of either QSOs. The measured *i* magnitudes (AB system) of the nucleus and of the host galaxy are reported in Table 3, together with the rest-frame Vega M_R absolute magnitude, dereddened and *k*-corrected. Corrections for galactic extinction were taken from SDSS data base and *k*-corrections from

[1] http://www.cfa.harvard.edu/castles/
[2] http://www-utap.phys.s.u-tokyo.ac.jp/~sdss/sqls/index.html

Table 1. Properties of low-redshift QSO pair sample.

Pair Nr (a)	A (b)	z_A (c)	i_A (mag) (d)	B (e)	z_B (f)	i_B (mag) (g)	$\Delta\theta$ (arcsec) (h)	$R_\perp$ (kpc) (i)	$\Delta V_\parallel$ (km s^{-1}) (j)
1	J001103.18+005927.2	0.4865	19.75	J001103.48+010032.6	0.4864	20.62	652	390	19 ± 28
2	J022610.98+003504.0	0.4240	19.54	J022612.41+003402.2	0.4239	19.09	66.0	360	25 ± 24
3	J074759.02+431805.3	0.5011	18.84	J074759.65+431811.4	0.5017	19.09	8.9	60	123 ± 18
4	J081801.47+205009.9	0.2357	17.45	J081808.77+204910.1	0.2356	18.81	118.1	440	36 ± 16
5	J082439.83+235720.3	0.5353	18.71	J082440.61+235709.9	0.5368	18.61	15.5	90	294 ± 19
6	J084541.18+071050.3	0.5376	18.73	J084541.52+071152.3	0.5352	18.60	62.3	390	468 ± 51
7	J085625.63+511137.0	0.5420	18.38	J085626.71+511117.8	0.5432	19.18	22.5	140	148 ± 21
8	J095137.01−004752.9	0.6340	20.23	J095139.39−004828.7	0.6369	20.02	49.8	350	544 ± 23
9	J113725.69+141101.3	0.7358	20.03	J113726.12+141111.4	0.7372	20.53	12.4	90	238 ± 28
10	J114603.49+334614.3	0.7642	20.11	J114603.76+334551.9	0.7615	19.23	23.3	170	445 ± 38
11	J124856.55+471827.7	0.4386	18.62	J124903.33+471906.0	0.4386	18.30	79.4	450	4 ± 15
12	J133046.35+373142.8	0.8141	19.32	J133048.58+373146.6	0.8144	19.82	26.4	200	54 ± 43
13	J155330.22+223010.2	0.6413	18.22	J155330.55+223014.3	0.6422	20.65	5.9	40	175 ± 12
14	J222901.08+031139.8	0.8069	21.69	J222902.03+031024.7	0.8087	19.88	76.5	570	299 ± 19

Notes. (a) Pair identification number. (b) and (e) SDSS QSO name. (c) and (f) QSO redshifts derived from [O III] line positions. (d) and (g) *i*-band apparent magnitude of the QSO A and B, respectively. (h) Angular separation of the pair. (i) Proper traverse separation $R_\perp$. (j) Radial velocity difference.

Table 2. Measurements of [O III]λ5007 Å emission lines based on the median of the barycentre of the line (see the text).

Pair Nr (a)	$\lambda_{[O\,III]}$ (A) (Å) (b)	$\lambda_{[O\,III]}$ (B) (Å) (c)
1	7442.47 ± 0.63	7441.99 ± 0.26
2	7129.84 ± 0.44	7129.24 ± 0.32
3	7515.70 ± 0.26	7518.77 ± 0.30
4	6187.15 ± 0.24	6186.41 ± 0.22
5	7686.78 ± 0.37	7694.31 ± 0.26
6	7698.28 ± 0.30	7686.28 ± 1.27
7	7722.53 ± 0.47	7726.33 ± 0.20
8	8180.92 ± 0.06	8195.76 ± 0.61
9	8690.95 ± 0.33	8697.85 ± 0.70
10	8832.83 ± 1.10	8819.75 ± 0.04
11	7202.80 ± 0.05	7202.88 ± 0.32
12	9082.84 ± 0.41	9084.48 ± 1.22
13	8217.60 ± 0.26	8222.40 ± 0.07
14	9047.04 ± 0.37	9056.06 ± 0.39

Notes. (a) Pair identification number. (b) and (c) Emission line centres of [O III]λ5007 emission line for QSOs A and B, respectively.

templates of Mannucci et al. (2001) and Francis et al. (2001) for host galaxies and nuclei, respectively.

The average absolute magnitudes M_R(nuc) of the nuclei is -23.0 ± 1.1 (median -23.1 ± 0.7), similar to the nuclear luminosities of isolated QSOs (e.g. Falomo et al. 2014). We find that the absolute magnitude M_R(host) of the host galaxies range between -21 and -24.5 (mean -22.9 ± 0.8; median -22.9 ± 0.5). The distribution of M_R(host) is comparable within similar redshifts to that reported for QSOs that are not in pairs (Falomo et al. 2014), indicating that the two families of QSO (individuals and in pairs) are indistinguishable from this point of view. Note that for ∼60 per cent of the objects the observations in the *i* filter include the [O III] emission line. This might contaminate the measurement of the host galaxy luminosity (e.g. because of scattered light from the nucleus). However, the same effect would be present also in the case of single QSOs at similar redshifts.

4 GALAXY ENVIRONMENT OF THE QUASAR PAIRS

In order to characterize the QSO pair environments, we analysed the distribution of galaxies around the QSOs using SDSS DR10 catalogues. From these, we obtained position and photometry of galaxies by selecting all primary objects photometrically classified as galaxies. In each QSO pair field, we analysed the *i*-band surface distribution of the galaxies within a circular area of 15 arcmin radius, corresponding to a projected distance of 3.4 Mpc from the nearest pair ($z = 0.236$) and 9.3 Mpc from the farthest ($z = 0.807$).

To estimate the completeness of the SDSS galaxy catalogues we compared the differential number counts of detected galaxies as a function of the magnitude with the very deep galaxy count data available from the Durham University Cosmology Group.[3] In particular, for each field we considered as threshold the magnitude $m_{i,\,50\,\mathrm{per\,cent}}$ where the completeness of observed galaxies drops to 50 per cent of that expected from Capak et al. (2007; see Fig. 3).

The apparent *i*-magnitude thresholds are closely distributed around the mean value of 21.96 ± 0.09 and listed in Table 4 with the corresponding absolute *k*-corrected magnitudes. At these thresholds we can observe galaxies with magnitude M^*+2 at $z < 0.3$, M^*+1 at $z \lesssim 0.5$ and M^* at $z \lesssim 0.8$.

In order to study the galaxy environment we followed the procedure described by Karhunen et al. (2014). To evaluate the surface number density of galaxies in the background, $n_{\rm bg}$, we considered the galaxies with $i < m_{i,\,50\,\mathrm{per\,cent}}$ and projected angular distance between 7 and 15 arcmin from the mid-point of the QSO pair. This corresponds to a minimum distance from the QSO of ∼1.6 Mpc for the nearest target. The region was then divided into annuli with width of 1 arcmin and we compute $n_{\rm bg}$ as the median of the galaxy surface density of each annulus and the semi-interquartile range is assumed as scatter (see Table 4). Finally, for each QSO we counted the surface number density of galaxies in a number of annuli with width of 250 kpc around the target. The galaxy overdensity of the QSO environment is the ratio between this number density and that of the background. In order to take into account the contribution of

[3] Durham University Cosmology Group, references and data in http://astro.dur.ac.uk/∼nm/pubhtml/counts/counts.html

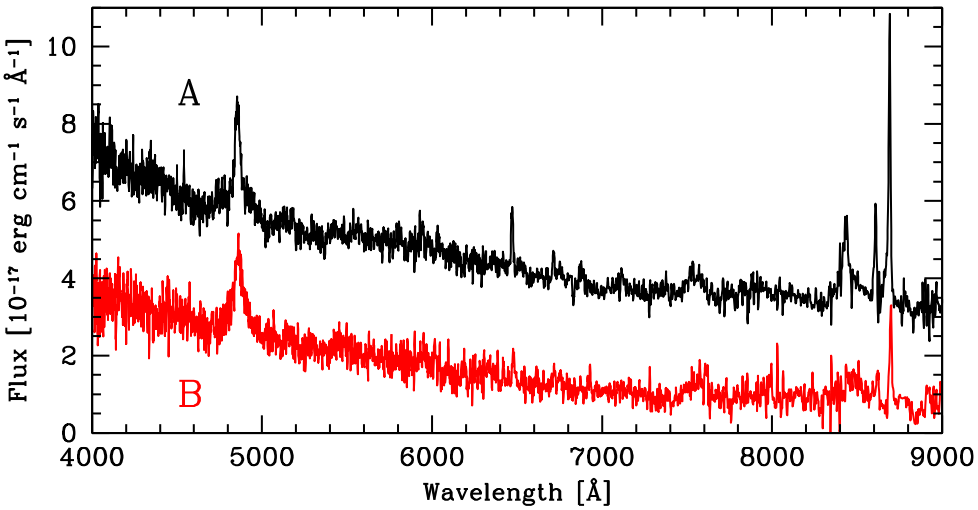

Figure 1. SDSS spectra of the QSOs in pair nr. 9 at $z = 0.736$. For clarity of comparison, the spectrum of the QSO A is shifted upwards.

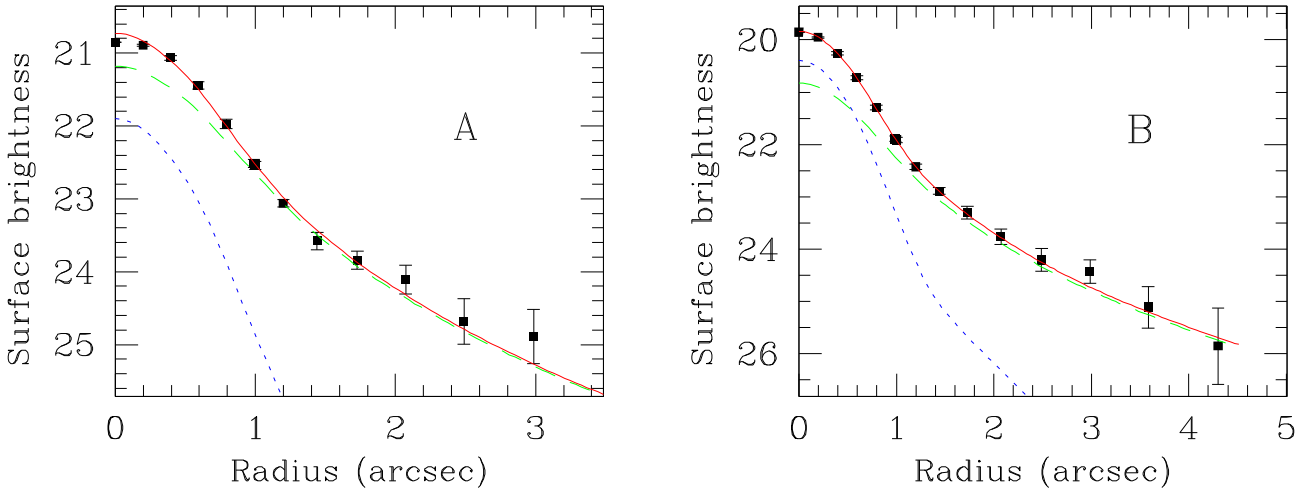

Figure 2. Examples of the QSO host galaxies decomposition for the QSO pair nr. 2. Left-hand panel: average radial brightness profile of the QSO A (square dots) fitted by the scaled point spread function (PSF) (dotted line) plus the host galaxy model convolved with the PSF (dashed line), see the text. The best fit is represented by the solid line. Right-hand panel: the same for the QSO B.

galaxies in the field around the QSO pair in the case that the annuli around the two QSO are overlapping, we have subdivided the excess galaxies in common to an equal number for each QSOs. The average cumulative overdensity distribution for the 28 QSOs is reported in Fig. 4, left-hand panel, and compared with that of isolated QSOs derived by Karhunen et al. (2014). We find that on average the galaxy overdensity around QSOs in pair is indistinguishable from that of isolated QSOs. For each QSO in our sample we report in Table 4 the galaxy overdensity inside a radius of 500 kpc.

It is of interest to probe whether the galaxy overdensity depends on the separation of the QSO pairs. To this aim, we computed the galaxy overdensity of the six pairs that are separated by less than 180 kpc and compare it with that expected under the assumption that each individual QSO contributes to the average value of galaxies (as given in Fig. 4, left-hand panel). The comparison (see Fig. 4, right-hand panel) suggests that closest QSO pairs may be in richer environments than those at larger separation. We performed a Kolmogorov–Smirnov (KS) test comparing the galaxy overdensity distribution of QSO pairs with $R_\perp < 180$ kpc to that of QSO pairs with larger separations. For the cumulative galaxy overdensity up to 1500 kpc the KS test yields the probability $p = 0.08$. This indicates that the suggestion should be confirmed by a significantly larger sample.

5 SUMMARY AND CONCLUSIONS

We have investigated the properties of the environments of a sample of 14 physical low-redshift QSO pairs. We found that the QSOs in pairs are on average in regions of modest galaxy overdensity extending up to ∼0.5 Mpc. This overdensity is indistinguishable from that of a homogeneous sample of isolated QSOs (Karhunen et al. 2014) that is matched in redshift and host galaxy luminosity. We note that for the closest QSO pairs there is a suggestion of a larger overdensity roughly commensurated to the sum of the average individual QSO environments.

Although the number of known QSO pair candidates (e.g. Hennawi et al. 2006; Myers et al. 2008) is much larger than that in our sample, a direct comparison with other results is at present not possible. For instance, the extended sample of QSO pairs of Hennawi et al. (2006) covers a wide redshift range (up to $z = 3$,

Table 3. Properties of nuclei and host galaxies.

QSO ID (a)	Class (b)	i_{nuc} (mag) (c)	i_{host} (mag) (d)	M_R(nuc) (mag) (e)	M_R(host) (mag) (f)	M(host) (10^{12} M$_\odot$) (g)
1A	R	19.90	21.61	−22.42	−21.07	0.09
1B	R	–	20.35	–	−22.33	0.3
2A	R	21.68	19.51	−20.38	−22.74	0.4
2B	R	20.16	19.03	−21.9	−23.22	0.7
3A	R	19.19	19.55	−23.23	−23.27	0.7
3B	R	19.45	19.90	−22.97	−22.94	0.5
4A	R	19.65	17.92	−20.64	−22.66	0.5
4B	R	19.29	19.68	−20.99	−20.90	0.09
5A	R	18.90	19.76	−23.65	−23.27	0.6
5B	M	18.77	20.43	−23.79	−22.61	0.4
6A	R	18.81	20.70	−23.74	−22.36	0.3
6B	M	18.72	20.53	−23.84	−22.51	0.3
7A	R	18.68	19.48	−23.86	−23.55	0.9
7B	U	19.17	–	−23.37	–	–
8A	R	20.50	19.98	−22.46	−23.64	0.9
8B	R	20.28	21.23	−22.7	−22.40	0.3
9A	U	20.08	–	−23.01	–	–
9B	R	21.32	21.03	−22.05	−23.15	0.5
10A	R	20.34	21.10	−23.13	−23.20	0.5
10B	R	19.25	19.69	−24.21	−24.59	1.9
11A	M	19.35	19.34	−22.75	−22.98	0.5
11B	U	18.31	–	−23.79	–	–
12A	M	19.43	21.01	−24.33	−23.51	0.7
12B	R	19.99	20.27	−23.66	−24.25	1.4
13A	R	18.29	20.04	−24.73	−23.65	0.9
13B	U	20.64	–	−22.39	–	–
14A	R	22.05	22.27	−21.75	−22.37	0.3
14B	M	19.99	21.97	−23.82	−22.68	0.3

Notes. (a) QSO identifier. (b) Resolved (R), marginally resolved (M), unresolved (U). (c) and (d) Apparent i magnitude (AB system) of the nucleus and host galaxy. (e) and (f) Absolute R-band magnitude (Vega system, k-corrected and dereddened) of the nucleus and host galaxy. (g) Mass of the host galaxy (see the text).

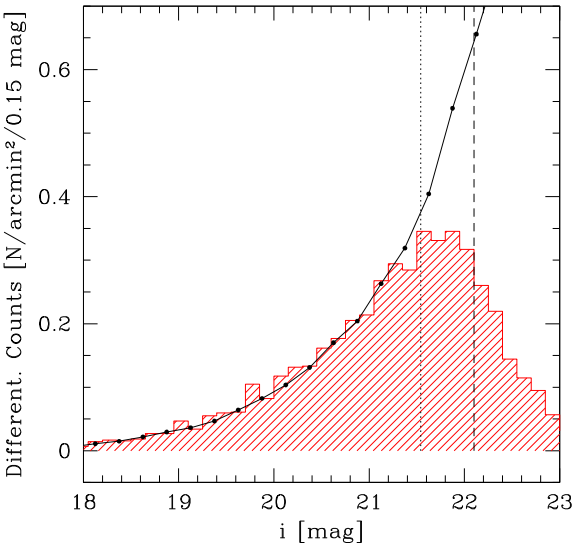

Figure 3. Number counts of galaxies as a function of i-magnitude in the field of QSO pair nr. 2 (shallow histogram). The black solid line represents for comparison the counts from deep survey of Capak et al. (2007). The dotted and dashed vertical lines mark the median magnitude and 50 per cent completeness threshold.

majority of pairs at $z > 1$), for which a detailed environmental study is not available and would require a major observational effort on large telescopes. Recently, Green et al. (2011) studied the environments around seven close QSO pairs ($R_\perp < 30$ kpc) in a redshift range comparable with ours. They searched for extended X-ray emission as evidence for a local group – or cluster – sized dark matter halo associated with these QSO pairs, and found none. In potential contrast to our results, they did not detect a significant optical/infrared galaxy density enhancement. Moreover, due to the relatively bright magnitude limits of SDSS images at the redshift of these pairs, only the most luminous galaxies possibly associated with the QSOs could be detected using their Distance and error-Weighted Colour Mean technique (Green et al. 2011). Within these limits, their results that QSO pairs avoid rich cluster environments are qualitatively in agreement with our findings.

Since the environment around pairs is relatively poor, it is of interest to compare it with the minimum mass of the binary system (the two QSOs) assuming it is gravitationally bound. Following F11, we computed the minimum virial mass associated with each pair and compared it with the total mass of the host galaxies (see Table 3), evaluated following Kotilainen et al. (2009) and Decarli et al. (2010). While in most cases $M_{vir,min}$ is less than or similar to the total mass of the host galaxies, in three cases (out of 14) $M_{vir,\,min}$ exceeds the sum of the masses of the hosts by a factor of $\gtrsim$10 (see

Table 4. Statistics of galaxy in the QSO pair environments.

Pair Nr (a)	$m_{i,\,50\,\mathrm{per\,cent}}$ (mag) (b)	$M_{i,\,50\,\mathrm{per\,cent}}$ (mag) (c)	n_{bg} (arcmin^{-2}) (d)	n_{bg} (Mpc^{-2}) (e)	$G_{0,\,5}(A)$ (f)	$G_{0,\,5}(B)$ (g)
1	21.9	−20.76	3.40 ± 0.10	26.20 ± 0.80	1.22 ± 0.04	0.68 ± 0.02
2	22.1	−20.14	4.01 ± 0.10	36.15 ± 2.71	1.14 ± 0.09	1.28 ± 0.10
3	21.9	−20.86	3.09 ± 0.16	23.16 ± 1.49	1.04 ± 0.12	1.04 ± 0.15
4	21.9	−18.62	2.24 ± 0.29	44.14 ± 6.02	0.89 ± 0.04	1.10 ± 0.04
5	21.9	−21.07	3.21 ± 0.09	22.30 ± 0.70	1.27 ± 0.07	1.21 ± 0.07
6	21.9	−21.08	3.27 ± 0.16	22.97 ± 1.39	0.87 ± 0.04	0.92 ± 0.07
7	21.8	−21.22	3.15 ± 0.15	21.98 ± 0.69	0.75 ± 0.15	0.87 ± 0.14
8	21.9	−21.67	3.06 ± 0.14	18.40 ± 0.59	1.11 ± 0.07	1.25 ± 0.05
9	22.0	−22.22	3.38 ± 0.16	17.85 ± 1.05	1.21 ± 0.04	0.93 ± 0.05
10	22.0	−22.41	3.41 ± 0.18	17.40 ± 1.02	1.27 ± 0.07	1.13 ± 0.07
11	22.0	−20.34	3.86 ± 0.10	33.88 ± 0.87	1.15 ± 0.04	1.07 ± 0.04
12	22.1	−22.68	4.56 ± 0.23	22.47 ± 0.98	0.88 ± 0.05	1.51 ± 0.06
13	22.0	−21.61	2.89 ± 0.27	17.05 ± 1.76	1.41 ± 0.02	1.33 ± 0.03
14	22.1	−22.63	4.10 ± 0.27	20.15 ± 1.47	0.57 ± 0.03	0.70 ± 0.03

Notes. (a) QSO pair identification number. (b) Apparent SDSS *i*-magnitude threshold. (c) Absolute magnitude corresponding to $m_{i,\,50\,\mathrm{per\,cent}}$. (d) and (e) Background surface number density of galaxies in arcmin^{-2} and in Mpc^{-2}, respectively. (f) and (g) Galaxy overdensity in the region within 500 kpc from the QSO, see the text.

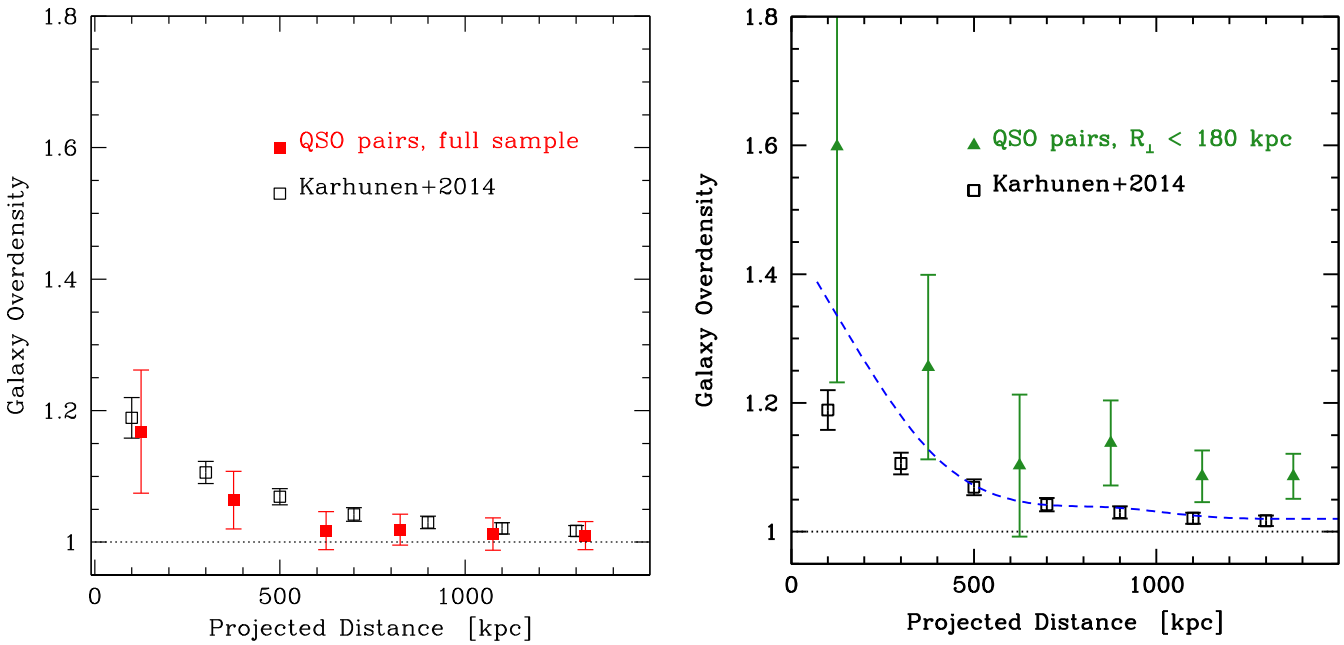

Figure 4. Left-hand panel: SDSS *i*-band mean cumulative overdensity of galaxies around the QSOs in pairs, corrected for the superposition of the companion environment (filled squares) as a function of the projected distance from the QSOs. Right-hand panel: same as the left-hand panel for whole QSO pairs with $0 < R_{\perp} < 180$ kpc (filled triangles). The expected galaxy overdensity around the whole QSO pairs, derived from the galaxy overdensity in the left-hand panel is plotted with the dashed line. In both the panels, the mean cumulative overdensity around isolated QSOs from the subsample at $i < 22$ mag derived by Karhunen et al. (2014) is plotted for a comparison (open squares).

Table 5). This is suggestive of a huge dark matter contribution (see also F11). However, because of the exiguity of our sample, to reach a firm conclusion on the environment and dynamical properties of QSO pairs, a detailed spectroscopic and imaging investigation of a larger and homogeneous sample is required.

ACKNOWLEDGEMENTS

We thank the referee for her/his constructive report which enabled us to improve our paper. We acknowledge the support of the Italian Ministry of Education (grant PRIN-MIUR 2010-2011).

Table 5. Comparison of the minimum virial mass of the QSO pairs with the total mass of their host galaxies.

Pair Nr (a)	$M_{\rm vir,\,min}$ ($10^{12}\,M_\odot$) (b)	$M_{\rm host,\,A}+M_{\rm host,\,B}$ ($10^{12}\,M_\odot$) (c)
1	(0.03 ± 0.09)	0.4
2	(0.05 ± 0.10)	1.1
3	0.20 ± 0.06	1.2
4	(0.13 ± 0.12)	0.6
5	1.9 ± 0.2	1.0
6	20 ± 4	0.6
7	0.7 ± 0.2	(1.7)
8	25 ± 2	1.2
9	1.1 ± 0.3	(1.0)
10	8 ± 1	2.4
11	(0.00 ± 0.02)	(1.1)
12	(0.14 ± 0.22)	2.0
13	0.30 ± 0.04	(1.8)
14	12 ± 2	0.6

Notes. (a) QSO pair identification number. (b) Minimum virial mass of the binary system. Values encompassed by bracket are not enough constrained. (c) Total mass of the QSO host galaxies in the pair. In the cases where only one QSO is resolved (see Table 3; in brackets), we consider the total mass to be twice that of the resolved QSO.

EPF acknowledges funding through the ERC grant Cosmic Dawn.

Funding for SDSS-III has been provided by the Alfred P. Sloan Foundation, the Participating Institutions, the National Science Foundation, and the U.S. Department of Energy Office of Science. The SDSS-III web site is http://www.sdss3.org/.

SDSS-III is managed by the Astrophysical Research Consortium for the Participating Institutions of the SDSS-III Collaboration including the University of Arizona, the Brazilian Participation Group, Brookhaven National Laboratory, Carnegie Mellon University, University of Florida, the French Participation Group, the German Participation Group, Harvard University, the Instituto de Astrofisica de Canarias, the Michigan State/Notre Dame/JINA Participation Group, Johns Hopkins University, Lawrence Berkeley National Laboratory, Max Planck Institute for Astrophysics, Max Planck Institute for Extraterrestrial Physics, New Mexico State University, New York University, Ohio State University, Pennsylvania State University, University of Portsmouth, Princeton University, the Spanish Participation Group, University of Tokyo, University of Utah, Vanderbilt University, University of Virginia, University of Washington, and Yale University.

REFERENCES

Ahn C. P. et al., 2014, ApJS, 211, 17
Bennert N., Canalizo G., Jungwiert B., Stockton A., Schweizer F., Peng C. Y., Lacy M., 2008, ApJ, 677, 846
Boris N. V., Sodré L., Jr, Cypriano E. S., Santos W. A., de Oliveira C. M., West M., 2007, ApJ, 666, 747
Callegari S., Kazantzidis S., Mayer L., Colpi M., Bellovary J. M., Quinn T., Wadsley J., 2011, ApJ, 729, 85
Capak P. et al., 2007, ApJS, 172, 99
Croom S. M. et al., 2005, MNRAS, 356, 415
Decarli R., Falomo R., Treves A., Kotilainen J. K., Labita M., Scarpa R., 2010, MNRAS, 402, 2441
Di Matteo T., Springel V., Hernquist L., 2005, Nature, 433, 604
Djorgovski S., 1991, in Crampton D., ed., ASP Conf. Ser. Vol. 21, The Space Distribution of Quasars. Astron. Soc. Pac., San Francisco, p. 349
Djorgovski S., Perley R., Meylan G., McCarthy P., 1987, ApJ, 321, L17
Djorgovski S. G., Courbin F., Meylan G., Sluse D., Thompson D., Mahabal A., Glikman E., 2007, ApJ, 662, L1
Ellingson E., Yee H. K. C., Green R. F., 1991, ApJ, 371, 49
Falomo R., Bettoni D., Karhunen K., Kotilainen J. K., Uslenghi M., 2014, MNRAS, 440, 476
Farina E. P., Falomo R., Treves A., 2011, MNRAS, 415, 3163 (F11)
Farina E. P., Montuori C., Decarli R., Fumagalli M., 2013, MNRAS, 431, 1019
Fisher K. B., Bahcall J. N., Kirhakos S., Schneider D. P., 1996, ApJ, 468, 469
Francis P. J., Drake C. L., Whiting M. T., Drinkwater M. J., Webster R. L., 2001, Publ. Astron. Soc. Aust., 18, 2
Green P. J., Myers A. D., Barkhouse W. A., Aldcroft T. L., Trichas M., Richards G. T., Ruiz Á., Hopkins P. F., 2011, ApJ, 743, 81
Hennawi J. F. et al., 2006, AJ, 131, 1
Hennawi J. F. et al., 2010, ApJ, 719, 1672
Hewett P. C., Wild V., 2010, MNRAS, 405, 2302
Karhunen K., Kotilainen J. K., Falomo R., Bettoni D., 2014, MNRAS, 441, 1802
Kormendy J., Fisher D. B., Cornell M. E., Bender R., 2009, ApJS, 182, 216
Kotilainen J. K., Falomo R., Decarli R., Treves A., Uslenghi M., Scarpa R., 2009, ApJ, 703, 1663
Liu X., Shen Y., Bian F., Loeb A., Tremaine S., 2014, ApJ, 789, 140
Mannucci F., Basile F., Poggianti B. M., Cimatti A., Daddi E., Pozzetti L., Vanzi L., 2001, MNRAS, 326, 745
McIntosh D. H., Guo Y., Hertzberg J., Katz N., Mo H. J., van den Bosch F. C., Yang X., 2008, MNRAS, 388, 1537
McLure R. J., Dunlop J. S., 2001, MNRAS, 321, 515
Myers A. D., Richards G. T., Brunner R. J., Schneider D. P., Strand N. E., Hall P. B., Blomquist J. A., York D. G., 2008, ApJ, 678, 635
Pâris I. et al., 2014, A&A, 563, A54
Porciani C., Magliocchetti M., Norberg P., 2004, MNRAS, 355, 1010
Schneider D. P. et al., 2010, AJ, 139, 2360
Serber W., Bahcall N., Ménard B., Richards G., 2006, ApJ, 643, 68
Silk J., Wyse R. F. G., 1993, Phys. Rev., 231, 293
Stockton A., 1978, ApJ, 223, 747
Uslenghi M., Falomo R., 2008, in Di Gesu V. et al., eds, Modelling and Simulation in Science. World Scientific, Hackensack, NJ, p. 313
Veron-Cetty M.-P., Veron P., 2000, VizieR Online Data Catalog, 7215, 0
Wake D. A. et al., 2004, ApJ, 610, L85
Yee H. K. C., Green R. F., 1984, ApJ, 280, 79
Yee H. K. C., Green R. F., 1987, ApJ, 319, 28
Zhdanov V. I., Surdej J., 2001, A&A, 372, 1

This paper has been typeset from a TEX/LATEX file prepared by the author.